Revista Brasileira de Física, Vol. 15, nº 2, 1985

Analysis of Strain Field Around β-Hydride in Nb-H by Electron Channelling

K. AKUNE

Departamento de Engenharia de Materiais, Universidade Federal de São Carlos, Caixa Postal 676, São Carlos, 13560, SP, Brasil

and

I.A.M. **BULHÕES**

Instituto de Física e Química de São Carlos, USP, Caixa Postal 369, São Carlos, 13560, SP, Brasil

Recebido em 15 de marco de 1985

Abstract The straín field in Nb-H system generated bythe precipitation of β-hydride has been evaluated quantitatively by Electron Channelling experiment. The results were analyzed in terms of the effective deformation of the Lëvi-Mises solid by making use of an elasto-plastic model of the strain field around the misfitting cylindrical precipitate.

1. IMRODUCTION

When high-energy electrons are incident on a crystal in the neighbourhood of a Bragg reflection, the electron state in the crystal can be described by a superposition of two bloch waves $B\ (\vec{r})$ and $B^{(2)}\ (\vec{r})$. Although both waves have the same energy, $B^{(1)}\ (\vec{r})$ is concentrated at the positions in-between the atoms while $B^{(2)}\ (\vec{r})$ at the positions of the atoms of the reflecting planes. The scattering coefficient for $B^{(2)}\ (\vec{r})$ will be greater than for $B^{(1)}\ (\vec{r})$ since in the former wave the maxima in the current are coincident with the scattering centers.

At the precise Bragg position, i.e. at $S=0$, where S indicates the deviation parameter from Ewald sphere, both Bloch waves are equally excited. At the positions $S<0$, $B^{(2)}\ (\vec{r})$ is preferentially excited. Consequently, for $S>0$ scattering is reduced and electrons channel into the lattice. For $S<0$ scattering is enhanced and the incidentelectrons are more back-scattered[1,2]. These facts cause the asymmetrical absorption of high-energy electrons on either side of the Bragg reflection and result in the formation of characteristic 1ine diffraction diagrams known as Electron Channellinq Patterns (ECP) in Scanning Electron Microscopy (SEM)[3]. Fig. 1 is an example of ECP in niobium.

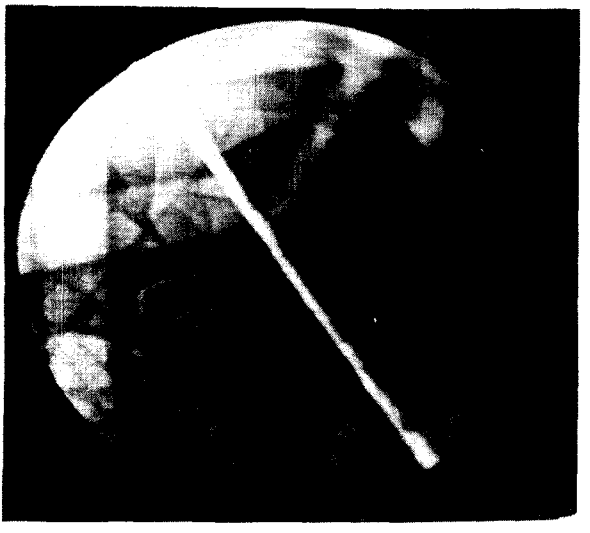

Fig.1 - ECP in niobium with β-hydride.

It is known that ECP line resolution, defined as the angular distance between the minimum and maximum intensity of ECP line, is closely related to the imperfections in the crystal such as dislocations, strain field and so on[4,5]. For example the authors have shown in their earlier work the linear relationship between ECP line resolution and deformation ratio in niobium[6]. The present work aims at evaluating the strain field in Nb-H generated by the misfitting precipitation of β--hydride by the technique of Electron Channelling (EC).

2. EXPERIMENTAL PROCEDURE

The niobium used in this study was obtained from Fundação de Tecnologia Industrial de Lorena in the form of a cylinder of approximately 5 mm in diameter and 11 mm in length.

The specimen was rapidly etched in a solution of 1HF + 1HNO_3 then annealed for 4 hours at 1500°C in a vacuum of 10^{-5} Torr. After cooling to room temperature, the specimen was equilibrated at 700°C with a controlled pressure of H_2 gas. The hydrogen concentration determined by a Leco RH_2 analyzer was found to be 760 ppm by weight. Fig. 2 shows the optical micrograph of the specimen thus prepared where the β-hydride

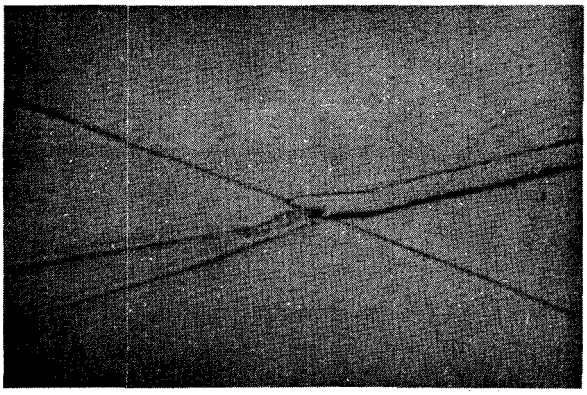

Fig.2 - Optical micrograph of Nb-H (X 70).

is seen in the form of lamellae.

The specimen was then introduced in a Scanning Electron Microscope (Cambridge S4-10) and EC experiment was performed with an accelerating voltage of 30 KV. The center of the electron beam spot was placed on the precipitate border and the spot diameter was changed approximately from 60 to 85 µm. Fig. 1 shows one of the ECP thus obtained. The resolution of the finest line, i e. the line having the highest Miller indices, was measured and converted into deformation ratio with a method described in detail elsewhere[6].

3. THEORETICAL BASIS*

We consider the precipitate as an isotropic cylindrical tube under the constraint of interna1 pressurepof matrix. It is expected that, because of a large volume change caused by the precipitation of β -Hydride ($\Delta V/V \sim 0,12$) [7], the strain field around the precipitate cansists of two zones: the elasto-plastic zone adjacent to the precipitate and the purely elastic zone. (Fig. 3).

The strain field around the cylindrical precipitate can be calculated in a way similar to the one used by Lee et *al.*[8] to calculate the strain field around a misfitting spherical precipitate. We use cylindrical coordinates (r,θ,z) whose origin is at the precipitate center as shown in F'ig. 3. We assume the matrix to be elastic, perfectly-plastic[9] and we neglect the crystallographic nature of plastic flow. The yielding

* As for the notations used in this section see the List of Symbols in the end.

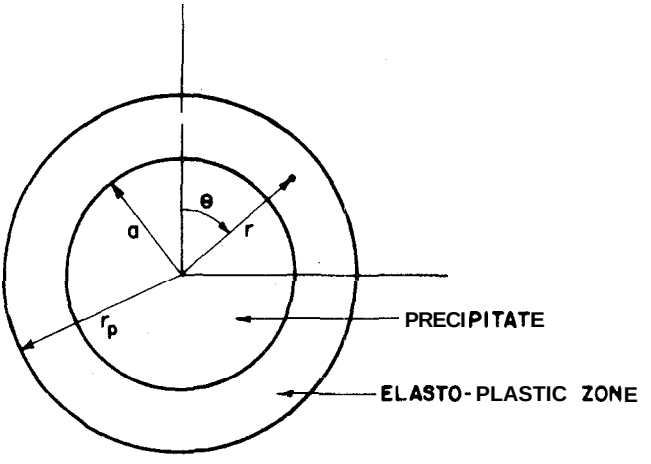

Fig.3 - Elasto-plastic zone and elastic zone surrounding a cylindrical precipitate.

of the matrix therefore takes place under the constant stress and is independent of the orientation of the stress axis.

We suppose also that the stress and strain do not depend on z and 8, i.e., their partial derivatives with respect to z and 8 are zero.

By the equilibrium condition in the absence of body force,

$$\frac{\partial \sigma_r}{r} + \frac{\sigma_r - \sigma_\theta}{r} = 0 \tag{1}$$

With the aid of Hook's law:

$$\begin{aligned} \sigma_r &= (\lambda+2\mu)\ \varepsilon_r + \lambda\ \varepsilon_\theta \\ \sigma_\theta &= \lambda\ \varepsilon_r + (\lambda+2\mu)\ \varepsilon_\theta \\ \sigma_z &= \lambda\ \varepsilon_r + \lambda\ \varepsilon_\theta \ , \end{aligned} \tag{2}$$

it can be shown that

$$\frac{\partial^2 u}{\partial r^2} + \frac{1}{r}\frac{\partial u}{\partial r} - \frac{u}{r^2} = 0 \tag{3}$$

where u is the radial displacement.

The general solution of (3) assumes the form

$$u = K_1\ r + \frac{K_2}{r} \tag{4}$$

where K_1 and K_2 are constants.

A. Pure Elastic State

We now suppose that the misfitting cylindrical precipitate, whose radius is $a(1+\varepsilon)$ in the absence of the matrix constraint, is inserted in a cylindrical hole of radius a and that its effective radius has become $a(1+\beta\varepsilon)$ under the matrix constraint (interna1 pressure p).

Then the boundary conditions on u are

$$u(r=a+) = \beta\varepsilon a$$
$$u(r=\infty) = 0 \quad , \quad \text{for the region } r>a \ ; \tag{5a}$$

$$u(r=a-) = (\beta-1)\varepsilon a$$
$$u(r=0) = 0 \quad , \quad \text{for the region } r<a \ . \tag{5b}$$

Inspection of (4) reveals that

$$u = \beta\varepsilon r \quad \text{for } r \leq a$$
$$\beta\varepsilon\, a^2/r \quad \text{for } r \geq a \tag{6}$$

It is clear that

$$u = (\beta-1)\varepsilon_r \qquad (0 \leq r \leq a) \tag{7}$$

(displacement in the precipitate)

and consequently,

$$\varepsilon_r^* = E_\theta^* = (\beta - 1)\varepsilon$$
$$\sigma_r^* = \sigma_\theta^* = 2(\lambda^* + \mu^*)(\beta - 1)\varepsilon \qquad (0 \leq r \leq a) \tag{8}$$

(elastic stress and strain in the precipitate)

where the superfix * refers to the precipitate phase.

The elastic stress and strain in the matrix can be written as

$$\varepsilon_r = \frac{\partial u}{\partial r} = -\beta\varepsilon \left(\frac{a}{r}\right)^2 = -\varepsilon_\theta \tag{9}$$

(elastic strain in the matrix)

Rook's law gives

$$\sigma_r = -2\mu\beta\varepsilon \left(\frac{a}{r}\right)^2 = -\sigma_\theta \tag{10}$$

(elastic stress in the matrix)

Inspetion of (10) reveals that

$$p = -2\mu\beta\varepsilon \tag{11}$$

Therefore (9) and (10) becorne

$$\varepsilon_r = -\varepsilon_\theta = -\frac{p}{2\mu}\left(\frac{a}{r}\right)^2 = -\left(\frac{1+\nu}{E}\right)\left(\frac{a}{r}\right)^2 \tag{9'}$$

$$\sigma_r = -\sigma_\theta = -p\left(\frac{a}{r}\right)^2 \tag{10'}$$

B. Elasto-Plastic Zone ($r_p \geq r \geq a$) and Elastic Zone ($r \geq r_p$)

As is shown later, the interna1 pressure p is large enough to cause yielding and consequently the plastic deforrnation takes place in the matrix adjacent to the precipitate. We adopt the Tresca yield criterion[9], i.e. yielding occurs when

$$\sigma_y = |\sigma_\theta - \sigma_r| \tag{12}$$

Then (1) reduces to

$$\frac{\partial\sigma_r}{\partial r} - \frac{\sigma_y}{r} = 0 \tag{13}$$

Considering the boundary condition

$$\sigma_r = -p \quad \text{at} \quad r = a ,$$

the solution of (13) is given by

$$\sigma_r = \sigma_y \log\left(\frac{r}{a}\right) - p \qquad a \leq r \leq r_p \tag{14}$$

(stress in the plastic region)

On the other hand, substitution of (10') into (12) results in

$$\sigma_y = 2p\left(\frac{a}{r}\right)^2 \tag{15}$$

Consequently, the yielding will start at the matrix-precipitate interface when the internal pressure reaches the critical value $\sigma_Y/2$, and as p increases the plastic zone of radius r_p will develop adjacent to the matrix-precipitate interface.

Now we calculate the stress in the elastic region of the matrix ($r \geq r_p$). By substituting the critical value $\sigma_Y/2$ for p and r_p for a in (10'), we obtain

$$\sigma_r = -\sigma_\theta = -\frac{1}{2}\sigma_y\left(\frac{r_p}{r}\right) \qquad (r \geq r_p) \tag{16}$$

(stress in the matrix in the elastic region)

By equating (16) and (14) at $r = r_p$, the plastic zone radius obtained:

$$r_P = a \exp\left\{\frac{p}{\sigma_Y} - \frac{1}{2}\right\} \tag{17}$$

(6), (10') and (11) yield the pure elastic deformation outside the plastic zone ($r \geq r_p$):

$$u = \frac{\sigma_y r_p^2}{4\mu}\frac{1}{r} \qquad (r \geq r_p) \tag{18}$$

(pure elastic deformation outside the plastic zone)

C. Strain in the plastic region

Within the plastic zone ($r_p \geq r \geq a$), strains are the sum of plastic and elastic strains. Since the elastic strains are related to Hook's law, we have

$$\begin{aligned}\varepsilon_r &= \frac{1}{E}\left[(1-\nu^2)\sigma_r - \nu(1+\nu)\sigma_\theta\right] + \varepsilon_r^p \\ \varepsilon_\theta &= \frac{1}{E}\left[(1-\nu^2)\sigma_\theta - \nu(1+\nu)\sigma_r\right] + \varepsilon_\theta^p\end{aligned} \tag{19}$$

where ε_r^p and ε_θ^p are the plastic strain components. Using the incompressibility condition[9]

$$\varepsilon_r^p + \varepsilon_\theta^p = 0 \tag{20}$$

and upon utilization of (19) and (12), we obtain

$$\frac{\partial u}{\partial r} + \frac{u}{r} = C_1 \log \left(\frac{r}{a}\right) + C_2 \tag{21}$$

where

$$C_1 = \frac{(1-\nu-2\nu^2) \cdot 2a\gamma}{E} \quad , \quad C_2 = \frac{(1-\nu-2\nu^2)(a-2p)}{E} \tag{22}$$

The differential equation (21) has a solution such as

$$u = \frac{1}{2} C_1 r \log \left(\frac{r}{a}\right) + \frac{1}{4}(2C_2 - C_1) r + C_3 \frac{r_p^2}{r} \qquad (a \leq r \leq r_p) \tag{23}$$

(deformation in the plastic region)

By equating (23) and (18) at $r = r_p$, C_3 can be determined:

$$C_3 = \left(\frac{1}{4\mu} + \frac{1-\nu-2\nu^2}{2E}\right) \sigma_y = \frac{1-\nu^2}{E} \sigma_y \tag{24}$$

Therefore the total (= elastic + plastic) strain is

$$\varepsilon_r = \frac{1}{2} C_1 \log \left(\frac{r}{a}\right) + \frac{1}{4}(2C_2 + C_1) - C_3 \left(\frac{r_p}{r}\right)^2 \tag{25}$$

$$\varepsilon_\theta = \frac{1}{2} C_1 \log \left(\frac{r}{a}\right) + \frac{1}{4}(2C_2 - C_1) + C_3 \left(\frac{r_p}{r}\right)^2 \tag{26}$$

The constants are given by

$$\frac{1}{2} C_1 = \frac{(1-\nu-2\nu^2)}{E} \sigma_y \quad , \quad \frac{1}{4}(2C_2 + C_1) = \frac{(1-\nu-2\nu^2)(\sigma_y - p)}{E} \quad , \quad \frac{1}{4}(2C_2 - C_1) = -\frac{(1-\nu-2\nu^2)p}{E} \tag{27}$$

We normalize the distance r with respect to the radius of precipitate a. Choosing the origin at the center of the electron beam spot, we define the $\zeta - \xi$ coordinate. (Fig. 4)

Then, setting $r/a \equiv 1+\zeta$, and $r_p \equiv na$, (24) and (25) reduce to

$$\varepsilon_r = \frac{1}{2} C_1 \log(1-\zeta) + \frac{1}{4}(2C_2 + C_1) - n^2 C_3 \frac{1}{(1-\zeta)^2} \tag{24'}$$

$$\varepsilon_\theta = \frac{1}{2} C_1 \log (1-\zeta) + \frac{1}{4} (2C_2 - C_1) + n^2 C_3 \frac{1}{(1-\zeta)^2} . \qquad (25)'$$

(24), (25) and (19) permit to calculate the plastic strain component:

$$\varepsilon_r^p = - \varepsilon_\theta^p = \frac{(1-\nu^2)\sigma_y}{E} \{1 - (\frac{r_p}{r})^2\} \quad (a \leq r \leq r_p) \qquad (28)$$

Finally, as the displacement should be continuous at $r = a$, (6) and (24) give the relation between p and $\beta\varepsilon$:

$$\beta\varepsilon = - \frac{(1-\nu-2\nu^2)}{E} + \frac{(1-\nu^2)\sigma_y}{E} \exp \left(\frac{2p}{\sigma_y} - 1 \right) \qquad (29)$$

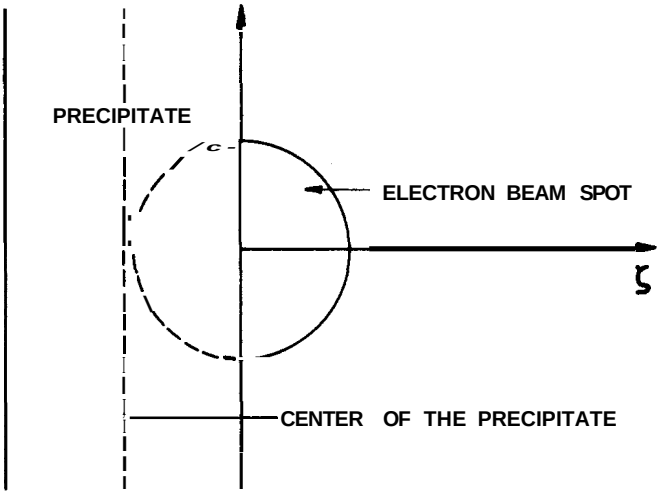

Fig. 4 - ζ - ξ coordinate.

4. ANALYSIS AND DISCUSSION

In Fig. 5 the deformation ratio estimated by EC is shown as vertical lines together with theoretical curves to be explained later. It should be noted that ECP line resolution (and consequently corresponding deformation ratio m) determined with the electron beam spot of radius ζ_0 is some average over the area 1/2 a ζ_0^2. As the defor-

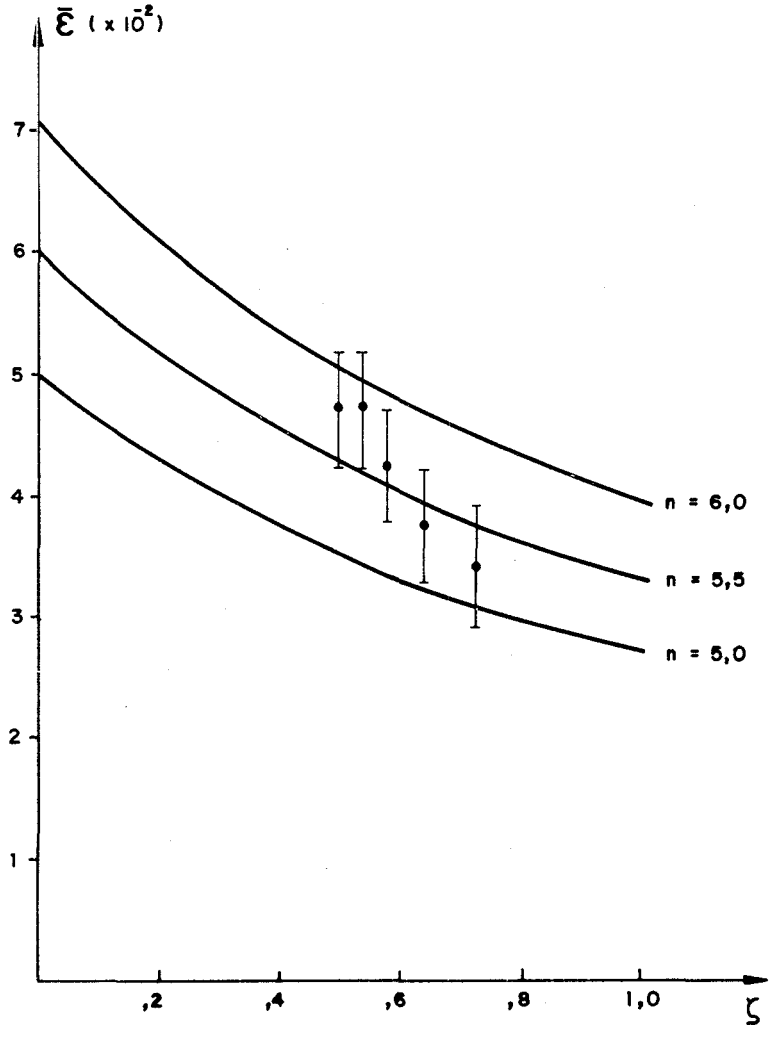

Fig. 5 - Deformation ratio detected by EC.

mation field is constant parallel to the precipitate border, $\overline{\varepsilon(\zeta)}$ may be written as

$$\overline{\varepsilon(\zeta_0)} = \frac{1}{1/2\ \pi\ \zeta_0^{\,2}} \int_{-\sqrt{\zeta_0^{\,2}-\zeta^2}}^{\sqrt{\zeta_0^{\,2}-\zeta^2}} d\xi \int_0^{\zeta_0} d\zeta$$

$$= \frac{4}{\pi\ \zeta_0^{\,2}} \int_0^{\zeta_0} \sqrt{\zeta_0^{\,2}-\zeta^2}\ \varepsilon(\zeta)\ d\zeta \qquad (30)$$

where $\varepsilon(\zeta)$ is the strain field felt by electron beam.

If rigid, and perfectly plastic behaviour of matrix is assumed, $\varepsilon(\zeta)$ may be expressed by the effective strain of Lévy-Mises solid[9]:

$$\varepsilon(\zeta) = \frac{2}{3}\sqrt{\varepsilon_r^{\,2} - \varepsilon_r\varepsilon_\theta + \varepsilon_\theta^{\,2}} \qquad (31)$$

With the aid of (24'), (25'), (30) and (31), we have made numerical calculus of $\varepsilon(\zeta_0)$ choosing several values of n*.

The continuous curves of Fig. 5 show the results. It is seen that the experimental results are fitted approxirnately by the curve corresponding to n = 5.5. In order to see the validity of the model, we calculated the value of $\beta\varepsilon$ by (29) and obtained $\beta\varepsilon$ = 0.50.

Since $\Delta V/V$ - 0.12, the expected value of $\beta\varepsilon$ is

$$(1+\beta\varepsilon)^2 - 1 = 0.12 \quad \text{i.e} \quad \beta\varepsilon = 0.58$$

In order to explain the discrepancy between experimental and theoretical values of $\beta\varepsilon$ and the deviation of experimental results from the theoretical curves in Fig. 5, we have considered the following causes: (1) yield criterion, (2) values of elastic moduli, and (3) influence of surface.

---

*The numerical values of elastic moduly used for the calculus are those given by Metal Handbook, American Society of Metals: ν = 0.38, $E = 1.03 \cdot 10^{12}$, $\mu = 3.75 \cdot 10^{11}$, $\sigma_y = 2.07 \cdot 10^9$ in c.g.s unit.

(1) Yield Criterion

The theory developed in section (3) makes use of the Tresca yield criterion. On the other hand, the results are analyzed with the aid of effective strain of Lévy-Mises solid which is equivalent to the Mises criterion. Therefore in order to maintain the consistency the theory should also be developed using the Mises criterion. However, the introduction of the Mises criterion makes most of the differential equations non-linear and the solutions cannot be obtained in terms of simple analytical functions. It is known that the Mises criterion gives higher value of yield stress a_Y than the Tresca criterion[9]. The use of the Mises criterion therefore might cause faster decrease of ε_r and ε_θ and consequently better accordance between the theoretical and experimental results might be expected.

(2) Elastic Moduli

The elastic moduli used in the analysis are values determined by some macroscopic experiment. Mathematically, the most appropriate values of elastic moduli are those averaged over all possible orientations of the coordinate system relative to the crystal axis. Two kinds of average are known, i.e., the Voigt average and the Reuss average, corresponding to the upper and lower bounds for compressibility and bulk modulus respectively* [10].

We calculated $\varepsilon(\zeta_0)$ using the values of elastic moduli given by the two averages. The results are best fitted by $n = 5.0$ for Voigt average and by $n = 5.0$ for Reuss average. The corresponding values of $\beta\varepsilon$ are 0.49 and 0.52 respectively. Therefore, in the range of theoretical upper and lower limits, the choice of elastic moduli affects relatively little the solution. The result that the Reuss average gives the closest value of $\beta\varepsilon$ to the theoretical one might be related to the fact

---

* for Niobium[10]

$\nu = 0.392$ $\mu = 3.96 \cdot 10^{11}$ $E = 1.10 \cdot 10^{12}$ Voigt average

$\nu = 0.336$ $\mu = 3.57 \cdot 10^{11}$ $E = 3.57 \cdot 10^{11}$ Reuss average

in c. g. s. units

(3) Surface Relaxation

In this study, the relaxation effect along the Z-axis and the influence of surface were neglected ($\partial/\partial\theta = 0$, $\partial/\partial Z = 0$). It may be therefore that the value of n is a little overestimated and that the real strain field decreases more rapidly than depicted in Fig. 5. This may also give rise to the deviation of the experimental results from the thereotical curves shown in the same figure, as well as the smaller value of $\beta\varepsilon$.

Finally, adopting the value n=5.5, the strain field around β--hydride was evaluated using (24') and (25') for the elastic moduli given in the page 13.

The results are shown in Fig. 6, where the total strain is described by the continuous curves and the plastic component by the dashed curves. The corresponding internal pressure p is estimated to be p - 2.2 σ_y from[17].

LIST OF SYMBOLS

σ_r	radial stress component
σ_θ	tangencial stress component
ε_r	radial strain component
ε_θ	tangencial strain component
σ_y	yield stress of matrix phase
β	constrained displacement parameter
ε	misfit parameter
E	Young's modulus
ν	Poisson's ratio
λ, μ	Lamé's constants
u	radial displacement

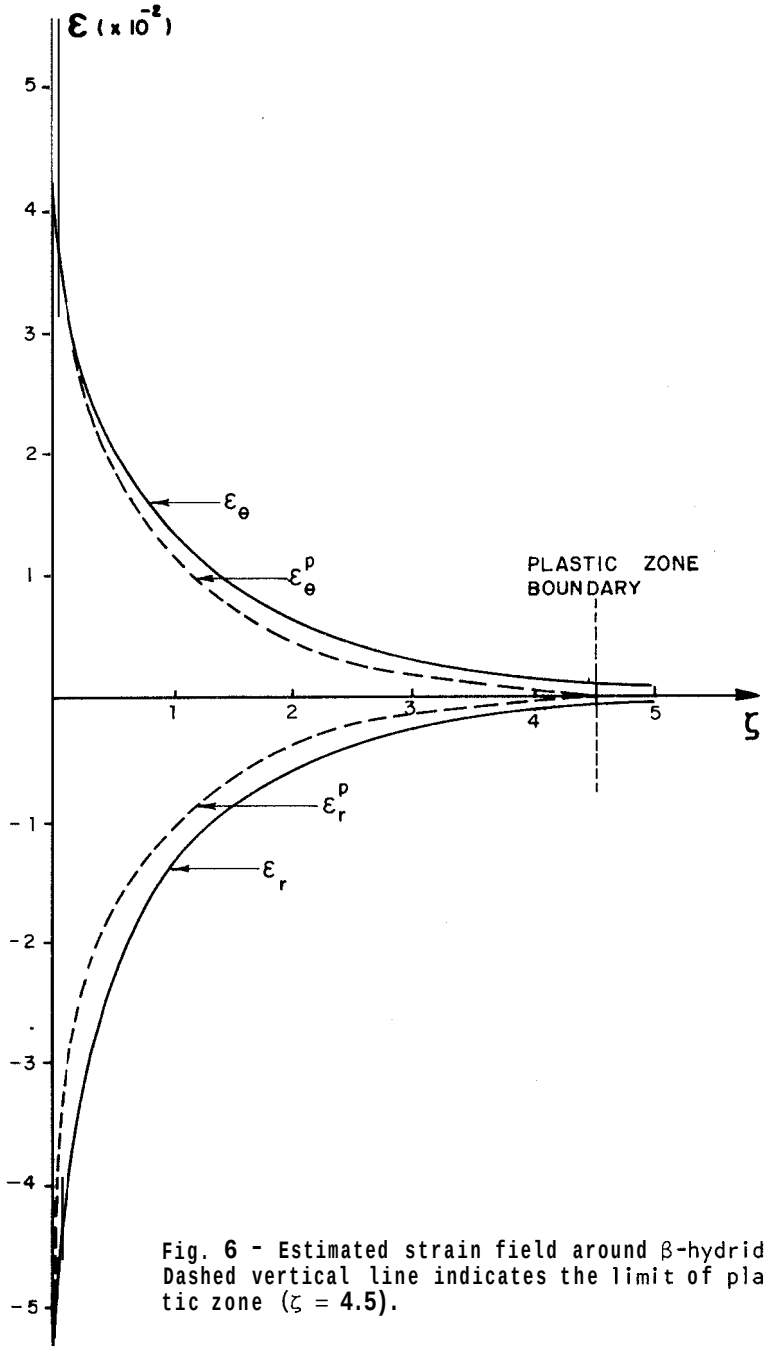

Fig. 6 - Estimated strain field around β-hydride. Dashed vertical line indicates the limit of plastic zone (ζ = 4.5).

REFERENCES

1. G.R. Booker, in *Modern Diffraction and Imaging Technique in Material Science,* (edited by S. Amelinckx, *et al.*) North Holland, Amsterdam (1970).
2. P.B. Hirsch, A. Howis, R.B. Nicholson, D.W. Pashley, M. J. Whelan, *Electron Microscopy of Thin Crystals,* Butterworths, London (1965).
3. E.M. Schulson, Proc. 25th EMAG Meeting, 286-300 (1971).
4. R. Stickler and G.R. Booker, Proc. 25th EMAG Meeting, 301-310 (1971).
5. D. C. Joy, *Quantitative Scanning Electron Microscopy*, Acad. Press., (1972).
6. I.A.M. Bulhões, K. Akune, D.G. Pinatti, Anais do XXXVI Congresso Anual da Associação Brasileira de Metais, Vol. 3, 325-333 (1981).
7. H.K. Birnbaum, M.L. Grossbeck and M. Amano, J. Less. Comm. Metals, 49, 357-370 (1976).
8. J.K. Lee, Y.Y. Earmme, H.I. Aaronson and K. C. Russel, Metall. Trans. *11*A, 1837-1847 (1981).
9. W. Johnson and P.B. Mellor, *Engineering Plasticity,* Van Nostrand Reinhold Comp., London (1973).
10. J.P. Hirth and J. Lothe, *Theory of Dislocations*, McGraw-Hill, Inc., New York (1968).

Resumo

Utilizando Tunelagem de Eletrons, foi avaliado quantitativamente o campo de tensão gerado pelos precipitados de hidreto-β no sistema Nb-H. Os resultados foram analisados em termos de deformação efetiva do sólido de Lévi-Mises, via a utilização de um modelo elasto-plástico do campo de tensões ao redor do precipitado.